Available online at www.sciencedirect.com
SCIENCE DIRECT®
Nuclear Physics A 739 (2004) 3–14
NUCLEAR PHYSICS A
www.elsevier.com/locate/npe

Study of the density distribution of ^{17}C from reaction cross section measurement

C. Wu [b,a,*], Y. Yamaguchi [a,c], A. Ozawa [a,1], R. Kanungo [a], I. Tanihata [a], T. Suzuki [d], D.Q. Fang [a,e], T. Suda [a], T. Ohnishi [a], M. Fukuda [f], N. Iwasa [g], T. Ohtsubo [c], T. Izumikawa [c], R. Koyama [c], W. Shinozaki [c], M. Takahashi [c]

[a] *Institute of Physical and Chemical Research (RIKEN), Hirosawa 2-1, Wako-shi, Saitama 351-0198, Japan*
[b] *School of Physics, Peking University, Beijing 100871, China*
[c] *Department of Physics, Niigata University, Niigata 950-2181, Japan*
[d] *Department of Physics, Saitama University, Saitama 338-8570, Japan*
[e] *Shanghai Institute of Nuclear Research, Chinese Academy of Sciences, Shanghai 201800, China*
[f] *Department of Physics, Osaka University, Toyonaka, Osaka 560-0043, Japan*
[g] *Department of Physics, Tokoku University, Sendai, Miyagi 980-8578, Japan*

Received 22 January 2004; received in revised form 4 March 2004; accepted 30 March 2004

Available online 15 April 2004

Abstract

The reaction cross section of ^{17}C on a carbon target at 79 A MeV has been measured by the transmission method. The density distribution of ^{17}C was deduced using the finite-range Glauber model (FRGM) combined with the interaction cross section of ^{17}C at high energy. The existence of a tail in the density distribution of ^{17}C is suggested to get a better understanding of both the low energy and high energy data. Under a core plus single-particle assumption, analysis shows a dominant d-wave of the valence neutron in ^{17}C.

PACS: 25.60.Dz; 21.10.Gv

Keywords: NUCLEAR REACTIONS C(^{17}C, X), $E = 79$ MeV/nucleon; measured reaction σ. ^{17}C deduced density distribution. Glauber model analysis.

* Corresponding author.
E-mail address: cuiewu@hep.pku.edu.cn (C. Wu).
[1] Present address: Institute of Physics, University of Tsukuba, Ibaraki 305-8571, Japan.

0375-9474/$ – see front matter
doi:10.1016/j.nuclphysa.2004.03.220

1. Introduction

The invention and development of the radioactive ion beam (RIB) has ushered in a new era on a variety of scientific research [1]. Investigations of the structure of exotic nuclei far from the stability line have attracted much interest in the past two decades. Measurements of interaction cross section (σ_I) or reaction cross section (σ_R) have been proved to be effective tools to reveal the halo or skin structure in proton-rich or neutron-rich nuclei [2–8].

For ^{17}C, the small one-neutron separation energy ($S_n = 0.729 \pm 0.018$ MeV) and large two-neutron separation energy ($S_{2n} = 4.979 \pm 0.018$ MeV) [9] support its possibility of being a one-neutron halo. However, recent work on the measurement of σ_I at relativistic energy has shown no halo structure in ^{17}C [5]. The same conclusion was drawn from work on one-neutron removal reactions [10]. In addition, a relatively broad momentum distribution (141 ± 6 MeV/c) of the fragment (^{16}C) was observed after one-neutron removal from ^{17}C [10–12].

A measurement of the momentum distribution of the core fragment (^{16}C) in coincidence with γ-rays from different excited states by V. Maddalena et al. was in good agreement with a theoretical prediction for a $J^\pi = 3/2^+$ assignment of the ground-state spin-parity of ^{17}C [13,14]. A measurement of the magnetic moment also concluded the $J^\pi = 3/2^+$ configuration [15]. The main component of the ground-state configuration was considered to be the $1d_{5/2}$ valence neutron coupled to the first excited state (2^+) of ^{16}C. An analysis for the Coulomb breakup of ^{17}C also yielded the same conclusion [16].

The reaction cross sections at lower energies around several tens of MeV/nucleon have been proven to be more sensitive to the nuclear density at the surface because of larger nucleon–nucleon total cross sections (σ_{NN}). Like ^{8}B, although measurements of σ_I at relativistic energies did not show a significant enhancement, measurements of σ_R at lower energy (around 40 A MeV and 60 A MeV) revealed the necessity of a long proton tail [4]. Based on this, in the present work, we measured the reaction cross section (σ_R) of ^{17}C on a carbon target at 79 A MeV using the transmission method. Together with previous data at high energy [5], we deduced the density distribution of ^{17}C by fitting the experimental data using the Glauber calculation.

2. Experiment

The experiment was performed at RIken Projectile fragment Separator (RIPS) of RIKEN Accelerator Research Facility [17]. Fig. 1 shows a schematic view of the experimental setup. A secondary beam ^{17}C was produced by the projectile fragmentation of the primary beam ^{22}Ne at 110 A MeV. The production target was beryllium (thickness $t = 2.5$ mm for reaction target-in runs and $t = 4$ mm for reaction target-out runs). At the first focus (F1), we put a wedge-shaped degrader (central thickness of 1244 mg/cm^2) and a PPAC (parallel plate avalanche counter) to determine the beam position, and also to give the start signal for a time-of-flight (TOF) measurement. A reaction target made of carbon ($t = 377$ mg/cm^2) was placed at the achromatic focus F2. Before the reaction target, two PPACs (F2PPACa and F2PPACb) were used to track incident nuclei and to obtain the beam

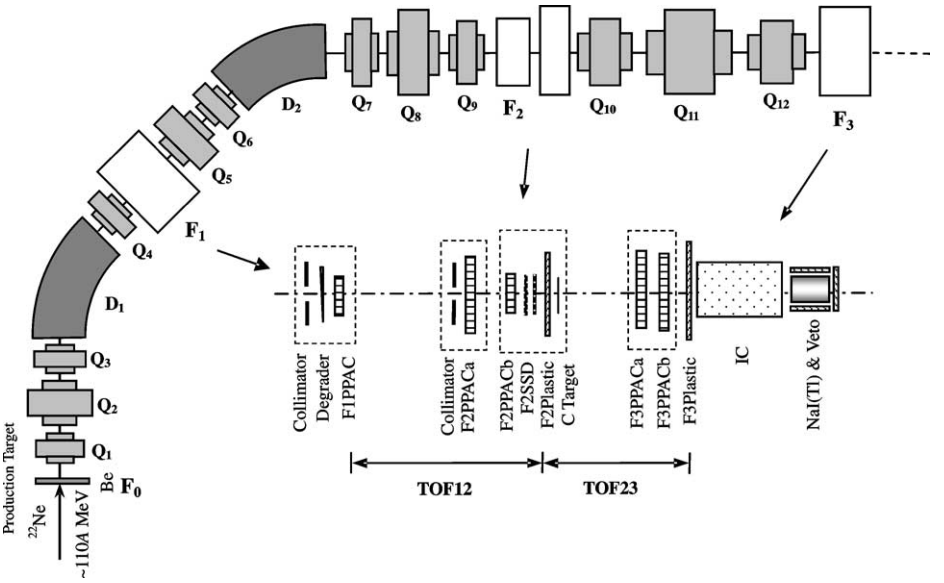

Fig. 1. Experimental setup at RIPS.

position and incident angle on the target. Particles before the reaction target were identified by the energy loss, ΔE ($\propto Z^2/v^2$) in Si detector (F2SSD, 156 μm), the TOF ($\propto 1/v$) between F1PPAC and F2Plastic (TOF12, flight length: ∼11.2 m, F2Plastic: $t = 0.5$ mm) and $B\rho$ ($\propto \frac{A}{Z} \cdot v$). The intensity of the ^{17}C beam at F2 was around 300 cps and the purity of ^{17}C was about 76%.

After the reaction target, all particles were transported by a quadruple triplet ($Q_{10–11–12}$) to F3. At F3, another two PPACs (F3PPACa and F3PPACb) were used to monitor the beam position. A scintillator (F3Plastic: $t = 1.5$ mm) was used to give the stop signal of TOF between F2Plastic and F3Plastic (TOF23, flight length: ∼4.9 m). An ion chamber (IC, $\phi = 90$ mm, length $l = 650$ mm) and NaI(Tl) were used to measure the energy losses (ΔE) and the total energies (E), respectively. Particles after the reaction target were identified by the TOF$-\Delta E - E$ method. In addition, we used a set of plastic counters as veto detectors around NaI(Tl) to detect the emitted charged particles or neutrons from reactions in NaI(Tl). After using veto rejection, fragments from reactions in the carbon target could be clearly separated from the background of reactions in NaI(Tl), as shown in Fig. 2.

3. Results

In this work, the transmission method was used to determine the reaction cross section. Two sets of data, with and without the reaction target, were taken. We define N_1 as the number of incident ^{17}C and N_2 as that of the outgoing unreacted ^{17}C. The reaction cross

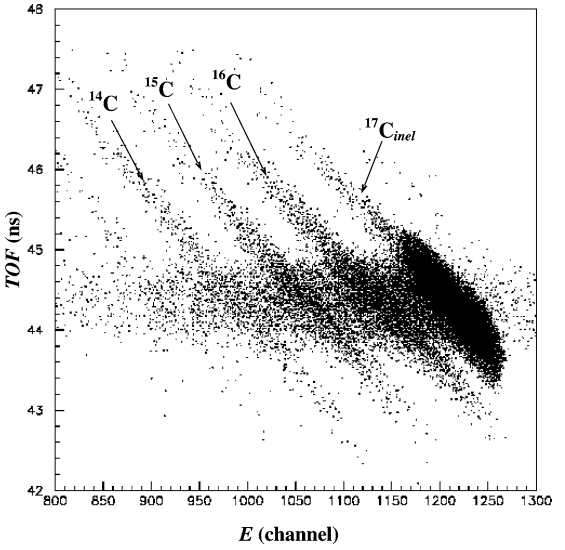

Fig. 2. Particle identification at F3 with $Z = 6$.

section can be determined by

$$\sigma_R = -\frac{1}{t}\ln\left(\frac{R_{\text{in}}}{R_{\text{out}}}\right), \tag{1}$$

where t is the thickness of the reaction target in atoms/cm^2 and $R = N_2/N_1$; subscripts *in* and *out* mean with and without the reaction target, respectively. The incident number of ^{17}C (N_1) was determined by particle identification before the reaction target. To determine N_2, the number of other fragments, N_{frag} (like ^{16}C, ^{15}C, ^{14}C, as can be seen from Fig. 2), and that of inelastic ^{17}C from reactions in the reaction target, N_{inel} (also shown in Fig. 2), should be subtracted from the total outgoing particles with $Z = 6$. The number of fragments (N_{frag}) was determined by subtracting the background of the target-out run from that of the target-in run after normalization with the total $Z = 6$ particles. The method used to determine N_{inel} is shown in Fig. 3.

First, we fit the tail of the inelastic part using an exponential function and extended it to the center of the peak, and then added a Gaussian tail with the same width as the main peak. We considered the number of events under this area as being the upper limit of N_{inel}, as shown by the vertical lines in Fig. 3. The lower limit of N_{inel} was estimated as being the number under the area of the exponential tail plus a linear decrease to zero at the center of the peak, as shown by the horizontal lines in Fig. 3. Finally, N_{inel} was determined to be the average of the upper and lower limits.

The present result of σ_R and the previous result of σ_I for ^{17}C are given in Table 1. The inelastic cross section (σ_{inel}) at the present energy was estimated to be (27 ± 15) mb. The uncertainties of the present measurement are discussed in the following and summarized in Table 2.

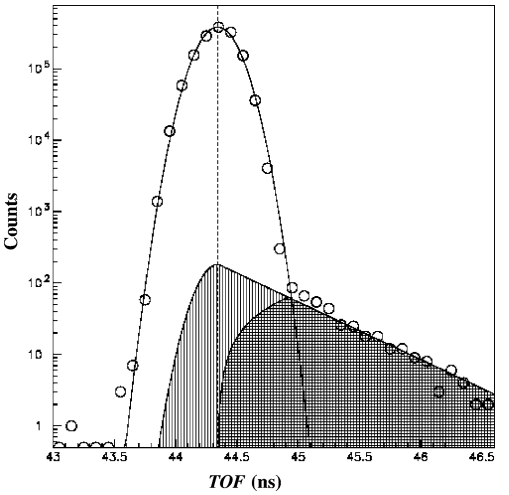

Fig. 3. Spectrum of inelastic events. The area with vertical lines and horizontal lines correspond to the upper and lower limits of inelastic events, respectively.

Table 1
Reaction cross section and interaction cross section of ^{17}C on carbon target

Energy (A MeV)	σ_R (mb)	σ_I (mb)	Reference
79	1350 ± 21	...	(present measurement)
965	...	1056 ± 10	[5]

Table 2
Experimental errors from the present measurement

Source	Contribution to error in σ_R (mb)
(1) Statistical	± 11
(2) Incident contaminations	± 9
(3) Estimation of fragments	± 4
(4) Target thickness	± 0.5
(5) Estimation of inelastic particles	± 15
Total	± 21

(1) The statistical error was one of the dominant uncertainties in σ_R, and was from the determination of N_2 for both reaction target-in and reaction target-out runs. We assumed that N_2 had a binomial distribution, and thus $\Delta N_2 = \sqrt{N_1 R(1-R)}$. The statistical error was then calculated by

$$\Delta\epsilon_{\text{stat}} = \frac{1}{t}\left(\frac{1-R_{\text{in}}}{N_{1\text{in}}R_{\text{in}}} + \frac{1-R_{\text{out}}}{N_{1\text{out}}R_{\text{out}}}\right)^{1/2}, \tag{2}$$

which gave an error of 11 mb in σ_R.

(2) Contamination of the incident beam, which could not be removed in the analysis, was a source of uncertainty in the number of incident particles. After selecting ^{17}C

using the $B\rho-\mathrm{TOF}-\Delta E$ method before the reaction target, the ratio of the number of contamination to that of the incident ^{17}C (r_{inci}) was 1.6×10^{-4}. The error from incident contaminations ($\Delta\epsilon_{\mathrm{inci}}$) was estimated as

$$\Delta\epsilon_{\mathrm{inci}} = -\frac{1}{t}\ln(1+r_{\mathrm{inci}}) \approx \frac{r_{\mathrm{inci}}}{t}, \tag{3}$$

which yielded an uncertainty of 9 mb in σ_R.

(3) Estimation of the number of fragments (N_{frag}) also gave an uncertainty to the final result. The statistical error of N_{frag} and the uncertainty from the subtraction method were taken into account, which corresponded to an uncertainty of 4 mb in σ_R.

(4) For the thickness of the reaction target, $\Delta t/t$ was measured to be 3.5×10^{-4}, which contributed a negligible error of 0.5 mb in σ_R.

(6) Another dominant uncertainty came from the estimation of inelastic events. We took half of the difference between the upper limit and the lower limit as the error of N_{inel}. This introduced an uncertainty of 15 mb in σ_R.

4. Analysis and discussion

4.1. Comparison with Kox formula

An energy-dependent, semiempirical formula to calculate the total reaction cross section for heavy-ion collisions was given by Kox et al. [18,19],

$$\sigma_R(E) = \pi r_0^2\left(A_P^{1/3}+A_t^{1/3}+a\frac{A_P^{1/3}A_t^{1/3}}{A_P^{1/3}+A_t^{1/3}}-C(E)\right)^2\left(1-\frac{V_{cb}}{E_C}\right), \tag{4}$$

where A_P and A_T are the mass number of the projectile and the target, respectively, $C(E)$ is the energy-dependent transparency parameter, V_{cb} is the Coulomb barrier of the projectile-target system and E_C is the kinetic energy of the projectile in the center-of-mass system. Parameters r_0 and a were determined by fitting the experimental data as $r_0 = 1.1$ fm and $a = 1.85$ fm.

As shown in Fig. 4, the present result of σ_R is much larger than that using the Kox formula. The enhancement of the experimental data to the Kox result at the present energy is also much larger than that obtained at high energy, which indicates the existence of a tail in the density distribution of ^{17}C.

4.2. Glauber model analysis

The Glauber model [20] has been widely used to deduce the density distribution, the root-mean-square (rms) radii and the momentum distribution of unstable nuclei [4,5,7,8, 21]. In the present work, we employed the finite-range Glauber model (FRGM) under the optical-limit approximation (for detailed description, see Ref. [8]).

The reaction cross section was calculated by

$$\sigma_R = 2\pi\int\left[1-T(b)\right]db\left(1-\frac{V_{\mathrm{cb}}}{E_C}\right), \tag{5}$$

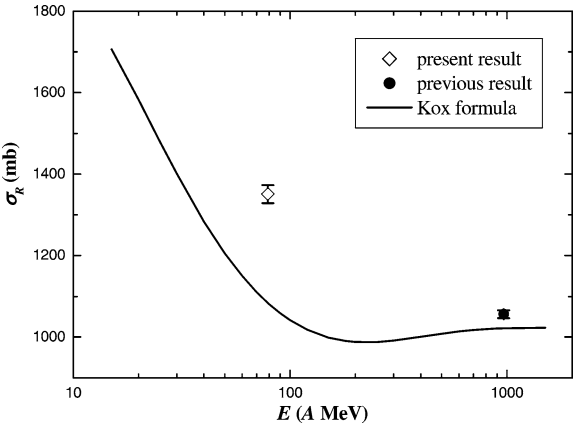

Fig. 4. Energy dependence of the cross section data. The solid line is a calculation using the Kox formula.

where $T(b)$ is the transmission at the impact parameter b, and is determined by the overlap of the density of the projectile and the target. The transmission ($T(b)$) is in the form of

$$T(b) = \exp\left\{-\int_P \int_T \sum_{ij} \left[\Gamma_{ij}(\boldsymbol{b}+\boldsymbol{s}-\boldsymbol{t})\rho^z_{Ti}(\boldsymbol{t})\rho^z_{Pj}(\boldsymbol{s})\right] d\boldsymbol{s}\, d\boldsymbol{t}\right\}, \tag{6}$$

where ρ^z_{Ti} and ρ^z_{Pj} are the z-direction integrated nucleon-density distributions of the target and the projectile; Γ_{ij} is the profile function, expressed as

$$\Gamma_{ij} = \frac{1-i\alpha}{4\pi\beta_{ij}^2}\sigma_{ij}\exp\left(-\frac{b_{ij}^2}{2\beta_{ij}^2}\right), \tag{7}$$

in which σ_{ij} is the total cross section of nucleon–nucleon collision and the range parameter (β_{ij}) is parameterized by fitting the $^{12}\mathrm{C} + {}^{12}\mathrm{C}$ reaction cross sections from 30 A MeV to 1 A GeV.

4.2.1. Fitting with HO density

Firstly we assumed a harmonic-oscillator (HO) density distribution for ^{17}C. The size parameter of HO (α_{HO}) was adjusted to fit the experimental data at high energy. The result of the FRHM calculation and the HO density are shown in Fig. 5. Large underestimation of the calculation was found at the present energy, which means that the simple HO density is not sufficient to describe the density distribution of ^{17}C.

4.2.2. Fitting with the (HO + Yukawa tail) density

Secondly, we assumed that the neutron density distribution of ^{17}C was composed of a HO core and a Yukawa tail at the outer region, as follows:

$$\rho_n(r) = \begin{cases} \mathrm{HO}(\alpha_{\mathrm{HO}}) & (r < r_c), \\ \rho_0 \exp(-\lambda r)/r^2 & (r \geqslant r_c). \end{cases} \tag{8}$$

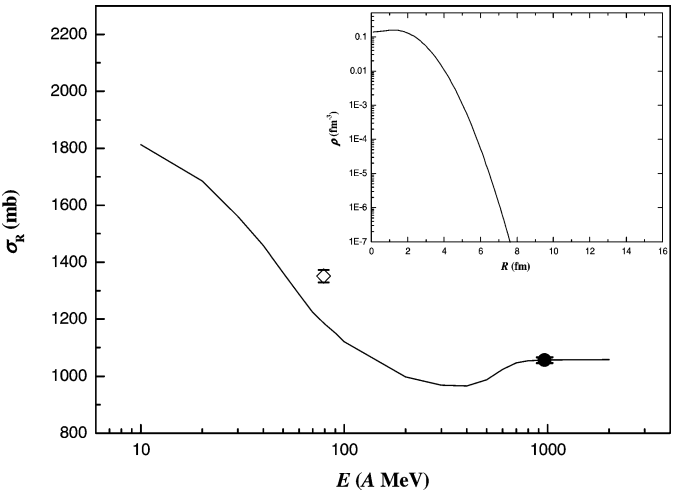

Fig. 5. The cross sections and the FRGM calculation with HO density shown in the inset.

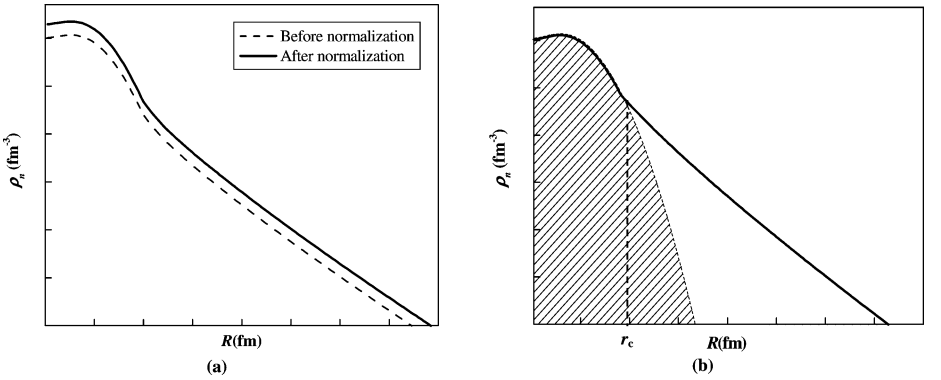

Fig. 6. Schematic diagram of the normalization method. (a) Norm.1; (b) Norm.2.

Here, r_c is the radius where the HO core crosses the Yukawa tail and λ is the slope of the tail. The proton density distribution of ^{17}C was assumed to be of the HO type with same α_{HO} as the neutron core.

Two normalization methods for the neutron density were used in the analysis, as schematically shown in Fig. 6. In the first method (Norm.1), there are three free parameters (α_{HO}, r_c and λ). The neutron density obtained with a specific set of these parameters was normalized to N, the total neutron number of ^{17}C (as shown in Fig. 6(a)). In the second method (Norm.2), there are two free parameters (α_{HO} and λ). As shown in Fig. 6(b), the shaded area is the HO density of the core with a width of α_{HO}, which was normalized to $(N-1)$. Thus, r_c could be determined by the total neutron density being normalized to N.

In the χ^2 fitting process, we assumed that α_{HO} (in Norm.1 and Norm.2) and r_c (in Norm.1) of ^{17}C were the same as those of ^{16}C [8]. The parameter λ was determined by the

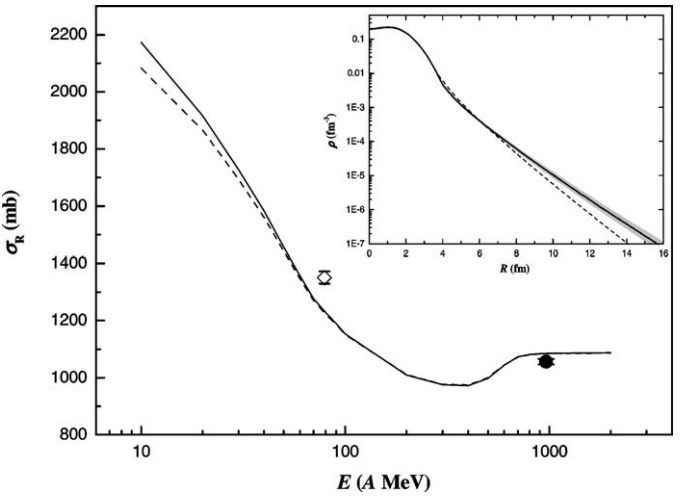

Fig. 7. The results of FRGM with the HO plus Yukawa tail densities shown in the inset: solid line, Norm.1; dashed line, Norm.2.

χ^2 minimization process for fitting both the experimental data. The result of the Glauber calculation and the supposed density of ^{17}C are shown in Fig. 7 with Norm.1 by the solid line and Norm.2 by the dashed line, respectively. It was found that the calculation with the HO plus Yukawa tail density agrees with the experimental data better than that with the HO density.

4.2.3. Fitting with (core + single particle) density

^{17}C is a typical p-sd shell nucleus. According to the naive shell model, the last three valence neutrons are expected to occupy $1d_{5/2}$. However, as mentioned in Refs. [1,7], the mixing of $2s_{1/2}$ and $1d_{5/2}$ has been found in many p-sd nuclei, such as ^{11}Li and ^{12}Be. Also, ^{15}C has an abnormal spin-parity of $1/2^+$, although it is expected to be $5/2^+$. Based on this phenomenon, we thirdly assumed that the neutron density of ^{17}C consisted of a ^{16}C core plus a neutron with a mixing of the s-wave and the d-wave. ^{16}C core was presumed to be at the first excited state, 2^+, to fulfill the $J^\pi = 3/2^+$ configuration of the ground state [15]. The core density was assumed to be the HO density, α_{HO} of which was obtained by fitting σ_I of ^{16}C at high energy [5]. The proton density of ^{17}C was supposed to be the HO density with the same α_{HO} as that of the neutron. The valence neutron density was calculated by the WAVEFUNC [22] code, in which a single-particle wave function was derived from a Woods–Saxon potential (radius parameter $r_0 = 1.22$ fm, diffuseness parameter $a = 0.7$ fm, same as in Ref. [5]) plus the Coulomb potential. In the calculation, we added the excitation energy (E_x) of the core to S_n. The potential depth was adjusted to reproduce $S_n + E_x$ ($0.729 + 1.766 = 2.495$ (MeV)).

We searched for the minimum χ^2 fit between the low energy and high energy data by varying the ratio of the s- and d-wave. A proportion of $77 \pm 21\%$ for the d-wave was found when the χ^2 reached the minimum. This means for ^{17}C, the d-wave is dominant (whereas, for ^{15,16,19}C [5,7,8], s-wave is dominant). This conclusion is consistent with the results of

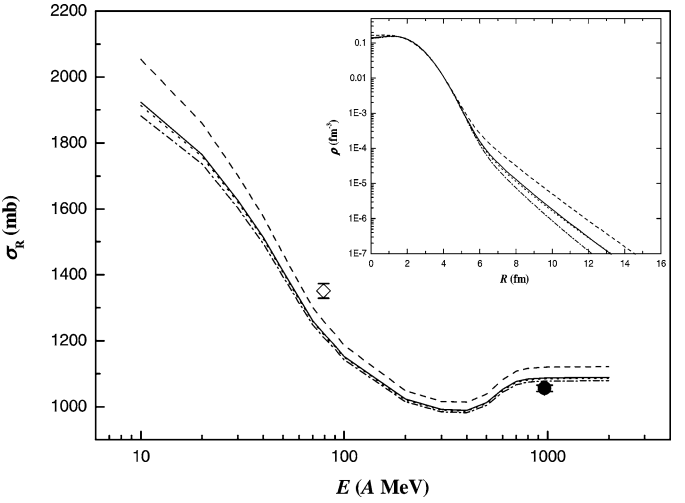

Fig. 8. The results of FRGM with the (core + single particle) densities shown in the inset: solid line, the mixture of 77% d-wave and 23% s-wave; dashed line, pure s-wave; dash-dotted line, pure d-wave; dotted line, with fixed parameters from Refs. [13,14,16].

Refs. [13,14,16]. The FRGM calculation with the mixture of d-wave (77%) and s-wave (23%) is shown in Fig. 8 by the solid line. The FRGM calculations assuming a pure $2s_{1/2}$ and a pure $1d_{5/2}$ neutron are also shown in Fig. 8 by the dashed and dash-dotted lines, respectively.

Construction of the density of ^{17}C was also tried using the (core + single particle) density combined with experimental information from Refs. [13,14,16]. The neutron density distribution of ^{17}C was assumed to be

$$\begin{aligned}\rho_n(r) = {} & A \times \left[{}^{16}\mathrm{C}\left(\mathrm{HO}, 0^+\right) \otimes \nu_{1d3/2}\right] \\ & + B \times \left[{}^{16}\mathrm{C}\left(\mathrm{HO}, 2^+\right) \otimes (a \times \nu_{1d5/2} + b \times \nu_{2s1/2})\right] \\ & + C \times \left[{}^{16}\mathrm{C}\left(\mathrm{HO}, 4^+\right) \otimes \nu_{1d5/2}\right], \end{aligned} \tag{9}$$

where all parameters ($A = 9\%$, $B = 64\%$, $C = 27\%$ and $a = 74\%$, $b = 26\%$) are fixed from Refs. [13,14,16]. The single-particle wave functions corresponding to the different excited states were obtained by using different binding energies in WAVEFUNC. The Glauber calculation and the constructed density are shown in Fig. 8 by the dotted line.

In conclusion, several methods used to probe the density of ^{17}C have been tried, as mentioned above. By assuming the HO plus Yukawa tail density of ^{17}C, the result calculated from FRGM agrees with the experimental data better than that with the HO density. The analysis of the (core + single particle) density supports d-wave dominance for the valence neutron of ^{17}C. It should be noted, however, that some discrepancy exists between the calculations using all density models and the experimental reaction cross section, which may be due to the deficiencies in the Glauber reaction theory at lower energies.

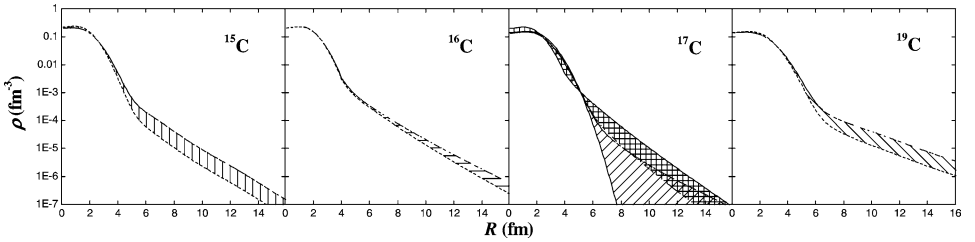

Fig. 9. Density distribution of carbon isotopes. The density of ^{17}C with crisscrossed lines is the present result and the others are from Refs. [5,8].

4.3. Density distribution of carbon isotopes

For a comparison, we plot (Fig. 9) the deduced density of ^{17}C of the present analysis together with the densities obtained for the carbon isotopes from Refs. [5,8]. For ^{17}C, we show the combination of the HO plus Yukawa tail density and the density from the (core + single particle) analysis by the crisscrossed lines. For ^{15}C, a recent analysis with all available σ_I and σ_R data showed a larger tail and supported an s-wave dominance [23]. Qualitatively, in most of the neutron-rich carbon isotopes, the density distribution of the tail derived from σ_I and σ_R shows a s-wave dominance. It is interesting to see that a similar study for ^{17}C suggests a dominance of d-wave.

5. Summary

In conclusion, we have measured the reaction cross section of ^{17}C on a carbon target at 79 A MeV using the transmission method. With the finite-range Glauber model, the density distribution of ^{17}C has been studied. Although the densities derived from several methods differ from one another, a tail in the density distribution of ^{17}C is suggested to obtain a better fit of the present reaction cross section and the interaction cross section at high energy. Based on the assumption of a core plus a neutron, it is found that the valence neutron of ^{17}C is mostly in the d-orbital, which is in agreement with the momentum distribution measurements [13,14,16]. In order to investigate the density distribution of ^{17}C precisely, more work on measurements of cross sections at other energies, especially at lower energies, are needed. The improvement of the theories for the study of low-energy nuclear reactions would be helpful to improve our understanding.

Acknowledgements

The authors gratefully acknowledge all of the staff at RIKEN Ring Cyclotron for their operation and technical maintenance during the experiment. One of the authors (Cuie Wu) is thankful to Prof. Y.L. Ye at Peking university for many valuable suggestions and to Dr. T. Zheng for sending the density distribution of ^{16}C data of Ref. [8] in a tabular form.

References

[1] I. Tanihata, Nucl. Phys. A 685 (2001) 80c.
[2] I. Tanihata, et al., Phys. Rev. Lett. 55 (1985) 2676.
[3] M. Fukuda, et al., Phys. Lett. B 268 (1991) 339.
[4] M. Fukuda, et al., Nucl. Phys. A 656 (1999) 209, and references therein.
[5] A. Ozawa, et al., Nucl. Phys. A 691 (2001) 599.
[6] A. Ozawa, et al., Nucl. Phys. A 693 (2001) 32.
[7] R. Kanungo, et al., Nucl. Phys. A 701 (2002) 378c.
[8] T. Zheng, et al., Nucl. Phys. A 709 (2002) 103.
[9] G. Audi, A.H. Wapstra, Nucl. Phys. A 595 (1995) 409.
[10] E. Sauvan, et al., Phys. Lett. B 491 (2000) 1.
[11] T. Baumann, et al., Phys. Lett. B 439 (1998) 256.
[12] D. Bazin, et al., Phys. Rev. C 57 (1998) 2156.
[13] V. Maddalena, et al., Phys. Rev. C 63 (2001) 024613.
[14] V. Maddalena, et al., Nucl. Phys. A 682 (2001) 332c.
[15] H. Ogawa, et al., Eur. Phys. J. A 13 (2002) 81.
[16] U. Datta Pramanik, et al., Phys. Lett. B 551 (2003) 63.
[17] T. Kubo, Nucl. Instrum. Methods B 70 (1992) 309.
[18] S. Kox, et al., Phys. Rev. C 35 (1987) 1678.
[19] L.W. Townsend, J.W. Wilson, Phys. Rev. C 37 (1988) 892.
[20] R.J. Glauber, in: W.E. Brittin, L.G. Dunham (Eds.), Lectures in Theoretical Physics, vol. 1, Interscience, New York, 1958, p. 315.
[21] T. Yamaguchi, et al., Nucl. Phys. A 724 (2003) 3.
[22] S. Hirenzaki, WAVEFUNC code, RIKEN, 1993.
[23] D.Q. Fang, et al., Phys. Rev. C 69 (2004) 034613.